Concentration and ion-energy-independent annealing kinetics during ion-implanted-defect annealing

R. Karmouch, J.-F. Mercure, Y. Anahory, and F. Schiettekatte[a)]
Regroupement Québécois sur les Matériaux de Pointe (RQMP), Département de Physique, Université de Montréal, C.P. 6128 succ, centre-ville, Montréal, Québec, H3C 3J7, Canada

(Received 4 June 2004; accepted 18 November 2004; published online 12 January 2005)

Nanocalorimetry revealed that the annealing kinetics of ion-implanted defects in polycrystalline Si is independent of ion fluence and implantation energy. Ion implantation of 30 keV Si^-, 15 keV Si^-, and 15 keV C^- was performed at fluences ranging from 6×10^{11} to 1×10^{15} atoms/cm^2, followed by temperature scans between 30 and 450 °C. The rate of heat release has the same shape for all fluences, featuring no peaks but rather a smooth, continuously increasing signal. This suggests that the heat release is dominated by the annealing of highly disordered zones generated by each implantation cascade. Such annealing depends primarily on the details of the damage zone–crystal interface kinetics, and not on the point defect concentration.
[DOI: 10.1063/1.1852733]

The evolution of defects in ion implanted crystalline Si upon thermal annealing continues to be the target of many investigations motivated by the scientific and technological relevance of this subject.[1] Ion implantation produces considerable lattice damage due to the energetic collisions of ions with lattice atoms. In monocrystalline silicon (*c*-Si), this results in an excess number of self-interstitials (I) that is responsible for phenomena such as transient enhanced diffusion, namely through {311} rod-like defect coarsening.[2] However, the structural evolution of point defects between room temperature (RT) and the onset of {311} defect formation around 680 °C is not fully understood. Experiments established that the kinetics of this evolution involves the agglomeration of point defect into clusters,[3] but these defect structures remain too small to be observed by microscopy, and too complex to be solved by spectroscopic methods. The latter can only identify and monitor the evolution of certain types of simple, electrically active defects, while ion implantation generates complex defect structures[4] that may not be observable by such techniques.

Another experimental approach to the problem is to look at the defect evolution from the thermal point of view. While calorimetry provide first-hand information about activation energies and heat exchanges during *all* thermal processes occurring in a sample, it has been the focus of only a few investigations. Differential scanning calorimetry (DSC) was performed on high-energy self-implanted Si[5] and high-energy H irradiated Si.[6] In this letter, we present nanocalorimetry experiments made on polycrystalline silicon (poly-Si) ion-implanted at low energy. It is shown that the rate of heat release has a very similar shape from very low to high fluences, which means that the annealing kinetics are independent of damage concentration.

Nanocalorimetry works on similar principles as DSC, but the scanning rate, reaching 10^6 K/s, and the resulting low thermal losses, make the technique orders of magnitude more sensitive to near-surface thermal processes. It has been able to considerably improve our understanding of a variety of systems, from the melting point depression in nanostructures[7] to the glass transition in thin polymer films.[8] The method is now applied *in situ* to defect dynamics in ion-implanted poly-Si.

A complete description of nanocalorimetry operation principles and the calculation method used to extract the heat capacity and latent heat of a deposited layer can be found in Refs. 9 and 10. Here, a 140 nm amorphous Si layer was deposited by Ar plasma sputtering on the 90-nm-thick SiN_x low-stress membrane of both sample and reference nanocalorimeters, in line with their Pt heating strips but on the opposite side of the membrane. Prior to the implantations, the nanocalorimeters were annealed at 900 °C for 100 s in a N_2 atmosphere to form a poly-Si layer. Transmission electronic microscopy (TEM) showed that the anneal produces crystallites of ~75 nm.

A sample and reference nanocalorimeter were then placed side by side in the implantation chamber with the sample poly-Si strip facing the beam, while the reference remained unimplanted. As material is deposited on *both* nanocalorimeters, heat capacity does not contribute to the signal, assuming they are identical. Actually, any difference in heat capacity between the nanocalorimeters is subtracted using a baseline measurement. The net result of the calculation[10] is thus the rate at which heat is released by damage annealing, in J/K.

Implantations of 30 keV Si^- (EOR=73 nm, 608 dpi), 15 keV Si^- (EOR=40 nm, 339 dpi) and 15 keV C^- (EOR =83 nm, 249 dpi) were performed, all at RT. The end-of-range (EOR) and displacements/ion (dpi) values are calculated from SRIM 2003 simulations.[11] Fluences expressed in displacements per atom (dpa) are calculated according to the number of atoms within the EOR.

After each implantation, ten nanocalorimetry scans were carried out by supplying a ~20 mA, 25 ms current pulse through the nanocalorimeters Pt heating strip, which resistively heated up at an average rate of 40 000 K/s. No measurable amount of heat was released after the first scan. A new set of nanocalorimeters was used for each series of implantations to avoid problems with possible damage accumulation.

[a)]Electronic mail: francois.schiettekatte@umontreal.ca

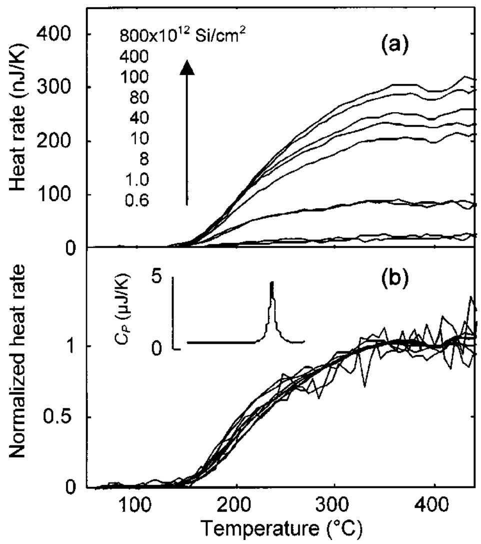

FIG. 1. (a) Rate of heat released by poly-Si implanted with 30 keV Si^- at indicated fluences. (b) Signals normalized by a factor proportional to the total heat released between 100 and 400 °C. Inset: melting peak of a 20 nm Sn layer, plotted on the same temperature scale as the data.

Figure 1(a) presents the heat rate curves obtained after implantations of 30 keV Si^- at fluences ranging from 6×10^{11} to 8×10^{14} Si^-/cm^2. It is seen that the heat increases more or less continuously with temperature. No feature that can be linked to simple first- or second-order processes such as point defect detrapping and recombination is revealed. This profile can rather be associated with processes characterized by a continuous distribution of activation energies. [As a comparison, the inset of Fig. 1(b) presents on the same temperature scale the signal obtained from the melting of 20 nm of Sn. Clearly, nanocalorimetry is capable of resolving fast features.] It is also seen that the total heat release increases with fluence, but not linearly. This is discussed in the following.

The crucial aspect revealed by these data is that the profile of the signal is similar at all fluences. In Fig. 1(b), the data are plotted with a normalization factor proportional to their integrated heat. It is seen that the signals superimpose surprisingly well, considering that the fluence range extends over more than three orders of magnitude. Comparable correspondence prevails for 15 keV C^- and Si^-. At a fluence of 6×10^{11} cm^{-2}, ion impacts are 13 nm apart on average. According to SRIM,[11] the average radius of the displacements distribution is 9.5 nm for 30 keV Si. (This is not the radial range provided by SRIM, but the displacements distribution considering individual cascades.) With 0.001 dpa, we are thus at the edge of a situation where cascades can be considered as isolated. Since the released heat has the same profile over the fluence range studied, it strongly suggests that the same kind of kinetics is going on in all cases. Therefore, for these low implantation energies, each individual cascade produces a kind of damage that is not different (or at least, that will not release heat differently) than the damage obtained after relatively high fluence implantation.

Such a continuous rate of heat release could be the result of the numerous point defect interactions forming different clusters and giving off heat all along the process. This hypothesis could be compared against simulations.[12] However, one can expect some change in the defect structures and associated kinetics when reaching high damage levels. Another possible explanation is that each cascade already produces heavily damaged zones that are complex enough so that their evolution translates into one that is not significantly different from what happens when cascades truly overlap each other, for instance after a fluence of 8×10^{14} Si^-/cm^2. Caturla *et al.* simulated by molecular dynamics the generation and evolution of damage induced by different ions implanted at low energy in Si.[4] They found that ion impacts result in so-called amorphous pockets, the size of which depends on the ion mass and energy. Their annealing is characterized by short (<10 ps) partial recrystallization steps. These steps are initiated by nucleation at the crystal interface and do not involve point defects. Moreover, Donnelly *et al.*[13] showed by TEM that the number of amorphous zones generated by 200 keV Xe implants at RT decreases monotonically with temperature. Zones with similar initial size do not even dissolve at the same temperature or rate. Recently, simulations by Nordlund *et al.*, including 10 keV Si recoils in Si, have also shown the formation of stable clusters containing more than 2/3 of the generated point defects.[14] Although these simulations were carried out at an equilibrium temperature of 0 K, it is clear that the annealing of a collection of highly disordered pockets is a good candidate to explain the continuous rate of heat release observed by nanocalorimetry. Smaller, shorter lifetime pockets are dynamically annealed at RT, causing the signal to start at zero, while larger ones are progressively annealed as the temperature rises. In this picture, cascade overlapping would not change significantly the annealing kinetics as it primarily depends on the details of the damage zone–crystal interface.[4]

Such interpretation also applies to DSC results obtained on *c*-Si irradiated with 8 MeV protons,[6] which show a heat release profile that features both peaks, and a broad background similar to what is observed here. The total heat released per dpa is comparable in both cases. Such irradiation does generate simple isolated Frenkel pairs through glancing angle collisions, but it also produces a significant number of primary recoils with energies of several kilo-electron-volts. While the peaks in the DSC signal are associated with simple point defect recombination processes, in view of the present results, the broad background may be attributed to the annealing of damage zones generated by these energetic recoils that are, in that case, truly isolated from each other.

Whether the presence of grain boundaries in the studied material influences the heat release remains an open question for the moment. If the heat release is mainly due to damage zone annealing, we expect no change when conducting the experiments in *c*-Si, considering the fairly large grain size in the material used here. In contrast, the heat release may be significantly affected by the presence of grain boundaries if the process depends on the details of single I–V interactions. I and V themselves should contribute to a relatively small amount of heat upon annealing.

The amount of heat released between 150 and 400 °C is presented in Fig. 2 for the different implanted ions and energies. These values are normalized to the number of atoms in the implanted depth (EOR). The dashed curve, fitted through low fluence data points, represents an increase proportional to $\varphi^{0.57\pm0.03}$, where φ is the fluence expressed in dpa. It shows that in all cases, the heat release increases sublinearly over the whole fluence range, saturating around a fluence of 1×10^{14} cm^{-2}, as seen from the inset. It is also clear from the figure that the results for the 30 and 15 keV

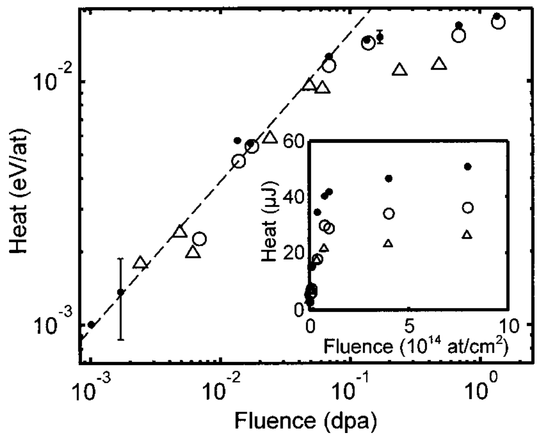

FIG. 2. Heat released between 150 and 400 °C by poly-Si implanted with 30 keV Si^- (●), 15 keV Si^- (○), and 15 keV C^- (△) as a function of fluence. The heat release is normalized to the number of atoms in the implanted region. Dashed curve: see the text. The inset shows the same data not normalized, and on a linear fluence scale.

Si^- implantations overlap. For the same fluence, the number of dpa is the same in both cases. It underlines that the annealing process is independent of implantation energy, at least in this energy range, and is not influenced by the surface. 15 keV C has nearly the same projected range as 30 keV Si, but produces 40% of the displacements. Figure 2 shows that at low fluences, C implantation generates the same amount of heat per atom as Si at the same dpa. At higher fluences though, the data depart from the results obtained for Si implantation to reach 70% of the signal. This stresses the nonlinearity of the process: displacements induced by C implantation are distributed more sparsely, in smaller defect structures, and are more susceptible to undergo dynamic recombination during the implant. Thus, the anneal will involve a smaller number of defects, releasing less heat. The fact that heavier ions generate a larger number of defects than predicted by binary collision simulations is outlined in Ref. 4, but here, the effect is seen only at high fluence, which indicates that cascade overlapping also comes into play for dynamic annealing. Meanwhile, the nanocalorimetry signals are at least qualitatively the same for C and Si implantation, so the underlying processes must be similar, and involve a wide spectrum of steps and activation energies.

In conclusion, it is shown that the kinetics of the heat release during ion implanted poly-Si annealing is independent of fluence and energy. Low energy, nearly isolated cascades readily produce a damage that releases heat the same way as heavy damage does. This strongly suggests that most of the rate of heat released during the annealing process can be described as a process internal to damage zones. As their annealing kinetics primarily depends on the details of the damage zone–crystal interface, the rate of heat release is independent of how distant cascades are from each other.

The authors are grateful to S. Roorda, R. Poirier, M. Chicoine, L. H. Allen, and M. Yu. Efremov for fruitful discussions. Thanks also go to L. Godbout and R. Gosselin for their technical assistance, Y. Q. Wang for TEM, M. Skvarla and P. Infante of the Cornell Nanofabrication Facility, as well as O. Grenier and S. Bah of the École Polytechnique de Montréal for their assistance with nanocalorimeters fabrication. This work benefited from the support of NanoQuébec, FQRNT, and NSERC.

[1] S. C. Jain, W. Schoenmaker, R. Lindsay, P. A. Stolk, S. Decoutere, M. Willander, and H. E. Maes, J. Appl. Phys. **91**, 8919 (2002), and references therein.

[2] B. Colombeau, N. E. B. Cowern, F. Cristiano, P. Calvo, N. Cherkashin, Y. Lamrani, and A. Claverie, Appl. Phys. Lett. **83**, 1953 (2003).

[3] N. E. B. Cowern, G. Mannino, P. A. Stolk, F. Roozeboom, H. G. A. Huizing, J. G. M. van Berkum, A. Claverie, F. Cristiano, and M. Jaraiz, Phys. Rev. Lett. **82**, 4460 (1999).

[4] M.-J. Caturla, T. Diaz de la Rubia, L. A. Marques, and G. H. Gilmer, Phys. Rev. B **54**, 16683 (1996).

[5] S. Roorda, W. C. Sinke, J. M. Poate, D. C. Jacobson, S. Dierker, B. S. Dennis, D. J. Eaglesham, F. Spaepen, and P. Fuoss, Phys. Rev. B **44**, 3702 (1991).

[6] R. Poirier, S. Roorda, F. Schiettekatte, M. Lalancette, and J. Zikovsky, Physica B **308-310**, 462 (2001).

[7] M. Yu. Efremov, F. Schiettekatte, M. Zhang, E. A. Olson, A. T. Kwan, R. S. Berry, and L. H. Allen, Phys. Rev. Lett. **85**, 3560 (2000).

[8] M. Yu. Efremov, E. A. Olson, M. Zhang, Z. Zhang, and L. H. Allen, Phys. Rev. Lett. **91**, 085703 (2003).

[9] M. Yu. Efremov, E. A. Olson, M. Zhang, F. Schiettekatte, Z. Zhang, and L. H. Allen, Rev. Sci. Instrum. **75**, 179 (2004).

[10] M. Yu. Efremov, E. A. Olson, M. Zhang, S. L. Lai, F. Schiettekatte, Z. S. Zhang, and L. H. Allen, Thermochim. Acta **412**, 13 (2004); R. Karmouch, J.-F. Mercure, and F. Schiettekatte, Thermochim. Acta (to be published).

[11] J. F. Ziegler, J. P. Biersack, and U. Littmark, *The Stopping and Range of Ions in Solids* (Pergamon, New York, 1985).

[12] L. Pelaz, G. H. Gilmer, V. C. Venezia, H.-J. Gossmann, M. Jaraiz, and J. Barbolla, Appl. Phys. Lett. **74**, 2017 (1999).

[13] S. E. Donnelly, R. C. Birtcher, V. M. Vishnyakov, and G. Carter, Appl. Phys. Lett. **82**, 1860 (2003).

[14] K. Nordlund, M. Ghaly, R. S. Averback, M. Caturla, T. Diaz de la Rubia, and J. Tarus, Phys. Rev. B **57**, 7556 (1998).